

FDG avid breast cancer bone metastases silent on CT and scintigraphy: a case report with radiologic-pathologic correlation

Daniel Jeong¹, Marilyn Bui^{2,3}, Daniel Peterson³,
Jaime Montilla-Soler¹ and Kenneth L Gage¹

Acta Radiologica Open
6(10) 1–7
© The Foundation Acta Radiologica
2017
Reprints and permissions:
sagepub.co.uk/journalsPermissions.nav
DOI: 10.1177/2058460117734243
journals.sagepub.com/home/arr



Abstract

Bone is the one of the most common distant metastatic sites in breast cancer. Routine initial breast cancer staging evaluation typically includes computed tomography (CT) and skeletal scintigraphy while 18F fluorodeoxyglucose (FDG) positron emission tomography-computed tomography (PET-CT) is reserved for clinically high-risk cases. Since FDG PET-CT is not routinely performed during staging or surveillance evaluations, it is important for radiologists and clinicians to appreciate the limitations of bone metastasis detection on CT and scintigraphy. We present a case of bony metastases of invasive ductal carcinoma of the breast which were not detected on diagnostic CT or skeletal scintigraphy but were metabolically active on FDG PET-CT and evident on magnetic resonance. We provide a review of the literature and radiologic–pathologic correlation to explain the discordant imaging findings.

Keywords

Breast neoplasms, bone neoplasms/secondary, PET-CT

Date received: 1 May 2017; accepted: 7 September 2017

Introduction

Bone is one of the most common distant metastatic sites in breast cancer. Approximately 70% of breast cancer patients develop bone metastases throughout the course of their disease, highlighting the importance of skeletal evaluation on staging and surveillance imaging to help prevent adverse skeletal related events (1). Current clinical guidelines from the National Comprehensive Cancer Network (NCCN) recommend consideration of additional imaging with computed tomography (CT) and skeletal scintigraphy in patients with stage I–IIIC invasive breast cancer. CT, skeletal scintigraphy, and magnetic resonance imaging (MRI) are also recommended for stage IV invasive breast cancer, whereas 18F fluorodeoxyglucose (FDG) positron emission tomography-computed tomography (PET-CT) has been proposed as an optional adjunct for clinically high-risk cases. Given these guidelines, it is important for radiologists and clinicians to appreciate the limitations of bone metastasis detection on CT

and scintigraphy (2). We present a case of bone metastases in invasive ductal carcinoma (IDC) of the breast, which were not detected on diagnostic CT or skeletal scintigraphy but were metabolically active on FDG PET-CT and evident on MRI. We review the literature and present radiologic–pathologic correlation to explain the discordant imaging findings.

¹Department of Diagnostic Imaging and Interventional Radiology, H. Lee Moffitt Cancer Center, Tampa, FL, USA

²Department of Anatomic Pathology, H. Lee Moffitt Cancer Center, Tampa, FL, USA

³Department of Cell Biology and Pathology, University of South Florida Morsani College of Medicine, Tampa, FL, USA

Corresponding author:

Daniel Jeong, Department of Diagnostic Imaging and Interventional Radiology, H. Lee Moffitt Cancer Center and Research Institute, 12902 USF Magnolia Drive, Tampa, FL 33612, USA.
Email: daniel.jeong@moffitt.org



Case report

A 47-year-old woman was diagnosed with a high-grade right breast IDC stage T3N2 which was immunohistochemically positive for estrogen receptor (ER), progesterone receptor (PR), and human epidermal growth factor receptor 2 (HER2). She underwent PET-CT, which showed a hypermetabolic lesion in the left sacral ala (SUVmax 4.4), which was not clearly visible on the accompanying CT or an ensuing three-month follow-up diagnostic multi-detector CT (MDCT) exam (Fig. 1a–d). This lesion did not have a sclerotic configuration and there was no associated cortical irregularity. Other FDG avid bone metastases were also noted in a right rib (Fig. 1e–h) and several vertebral bodies, without well-defined corresponding lesions on MDCT.

An accompanying negative Tc99m methylene diphosphonate (MDP) skeletal scintigraphy obtained one week following initial FDG PET-CT suggested absent osteoblastic activity in these breast cancer metastatic lesions (Fig. 2). Pelvic magnetic resonance (MR) was obtained one month after PET-CT to further evaluate the suspected bony metastases (Fig. 3). MR demonstrated a well-defined 0.9-cm enhancing lesion in the left sacral ala with mildly increased T1-weighted (T1W) and increased T2-weighted (T2W) signal and restricted diffusion. This sacral lesion was targeted for CT-guided biopsy using the FDG PET-CT with anatomic landmarks for guidance given the absence of a well-defined lesion on CT.

The left sacral biopsy gross specimen consisted of a cylindrical fragment of bone ($1.0 \times 0.8 \times 0.4$ cm). Following decalcification, hematoxylin and eosin (H&E) sections demonstrated replacement of normal bone marrow elements with an infiltrative neoplastic process consisting of epithelioid cells growing in cords with round monomorphic nuclei and occasional nucleoli (Fig. 4). The morphologic features were compatible with the previous right breast core needle biopsy displaying IDC, Nottingham combined histologic grade 3. Immunohistochemical studies on the sacral lesion supported this finding with the following positive immuno-stains: CK7, GATA3, ER, PR, and HER2.

For treatment of breast cancer, the patient was started on docetaxel, trastuzumab, and pertuzamab (THP) chemotherapy given HER2 positivity before these imaging studies. With detection of skeletal metastases on FDG PET-CT imaging, the patient also started denosumab therapy to reduce the risk of adverse skeletal-related events such as pathologic fracture or pain requiring intervention.

On three-month surveillance MDCT exam, there was significant improvement in the patient's breast and right axillary masses. However, the bone lesions remained poorly defined and were not clearly

visualized. Follow-up skeletal scintigraphy was unchanged without evidence of increased osteoblastic activity. No adverse skeletal events were encountered by the patient during this time.

Discussion

Breast cancer bone metastases are predominantly osteolytic, with only about 15–20% of patients having osteoblastic dominant metastases. While osteoblastic metastases are well visualized on CT due to the increased sclerotic density, lytic lesions can pose a challenge (3). Lytic lesions appear hypodense on CT and are circumscribed from surrounding bone marrow, while associated bony cortical destruction assists in delineating lesion boundaries (4). However, a minimum degree of cortical destruction is required for visualization of a lytic bone metastasis on CT, which can decrease the sensitivity of CT for early bone metastasis detection where only marrow is involved (5,6). The histologic juxtaposition of normal marrow and tumor cells in our patient may explain the subtlety of this lesion on CT (Fig. 4c). Although CT offers excellent anatomical resolution and soft-tissue contrast for morphologic evaluation, scintigraphy, MR, and FDG PET-CT have been suggested to be more sensitive in the detection of certain skeletal metastases (4,7).

Skeletal scintigraphy relies on the radiotracer Tc99m methyl diphosphonate, which enables evaluation of local bone turnover as MDP gets incorporated into hydroxyapatite of bone. Skeletal scintigraphy allows visualization of uptake in regions of increased bone turnover and osteoblast activity and a resulting increase in blood perfusion (8). The initial accumulation of seeded tumor cells in the intramedullary compartment leads to marrow replacement and tumor cell proliferation before the reactive osteoblastic response. Therefore, early or predominantly lytic lesions will be silent on scintigraphy. Skeletal scintigraphy is insensitive for tumors that are predominantly lytic, but even lytic tumors can be visualized if successful treatment leads to metabolic activation and bone matrix regeneration (8). Additionally, bone metastases in avascular sites of disease can also result in false-negative exams due to the lack of increased perfusion that typically accompanies osteoblastic activity (8,9).

MR has shown to be more sensitive than both CT and skeletal scintigraphy but less sensitive than FDG PET-CT for general bone metastases (10). The presence of neoplastic bone infiltrates causes increased T1 and T2 relaxation times resulting in clear signal changes on MRI (11,12). On FDG PET-CT, breast cancer bone metastases demonstrate increased glucose metabolism regardless of osteoblastic response, therapy increasing the sensitivity of PET-CT.

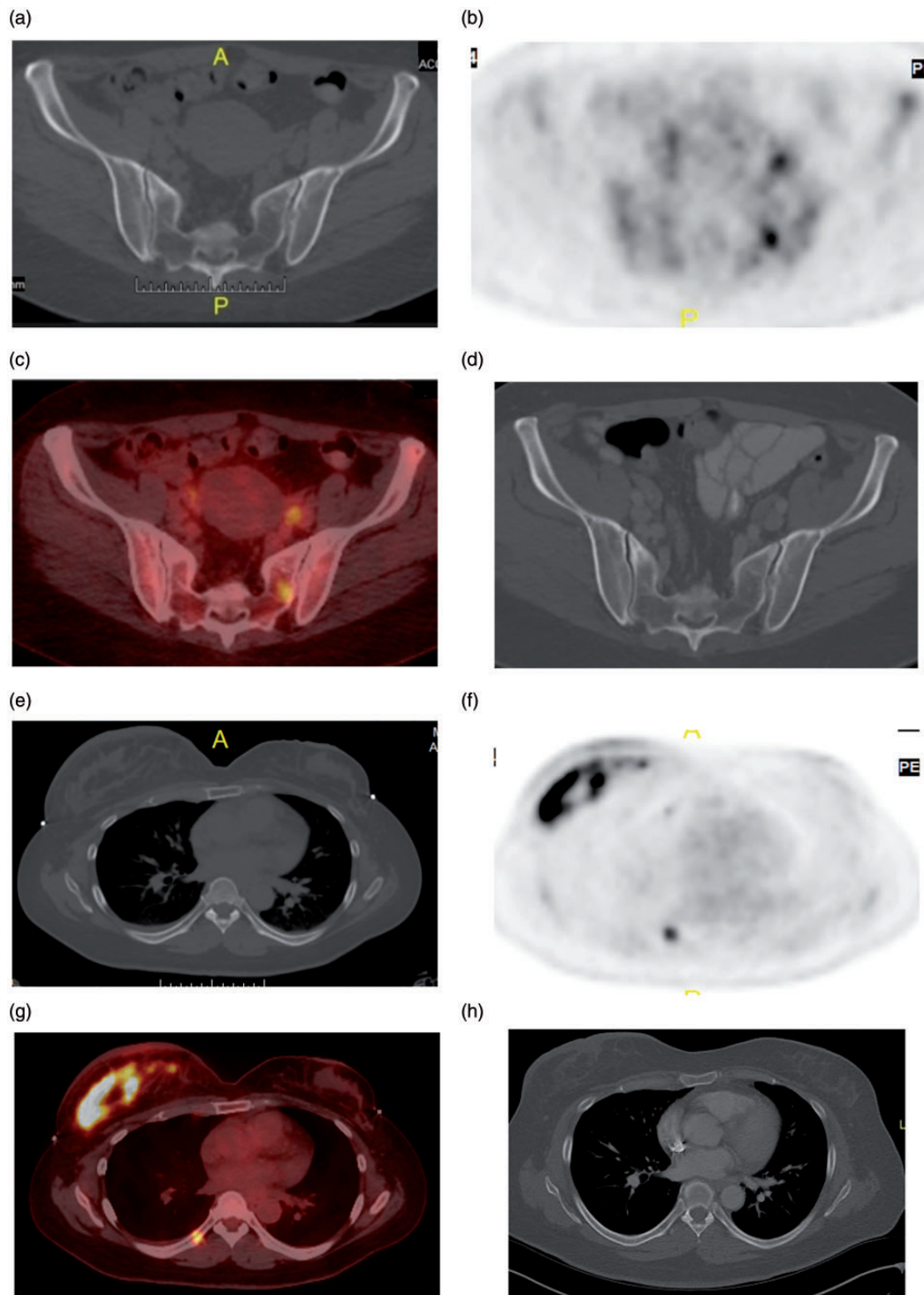


Fig. 1. (a) Axial CT image from FDG PET-CT acquisition shows no well-defined lesion corresponding to the site of FDG activity in the left lateral sacrum on (b) axial PET image. (c) Fused axial PET and CT image show FDG activity in the left sacrum without a well-defined lesion on CT. (d) Diagnostic MDCT at the corresponding site in the sacrum shows no definite cortical destruction. (e) Axial CT image from FDG PET-CT acquisition shows no well-defined lesion corresponding to the site of FDG activity in a posteromedial right rib on (f) axial PET image. (g) Fused axial PET and CT image show FDG activity in a right posterior rib without a well-defined lesion on CT. Also note the FDG avid right breast mass representing this patient's primary invasive ductal carcinoma. (h) Diagnostic MDCT at the corresponding site of right rib FDG activity shows no cortical destruction or well defined lytic lesion.

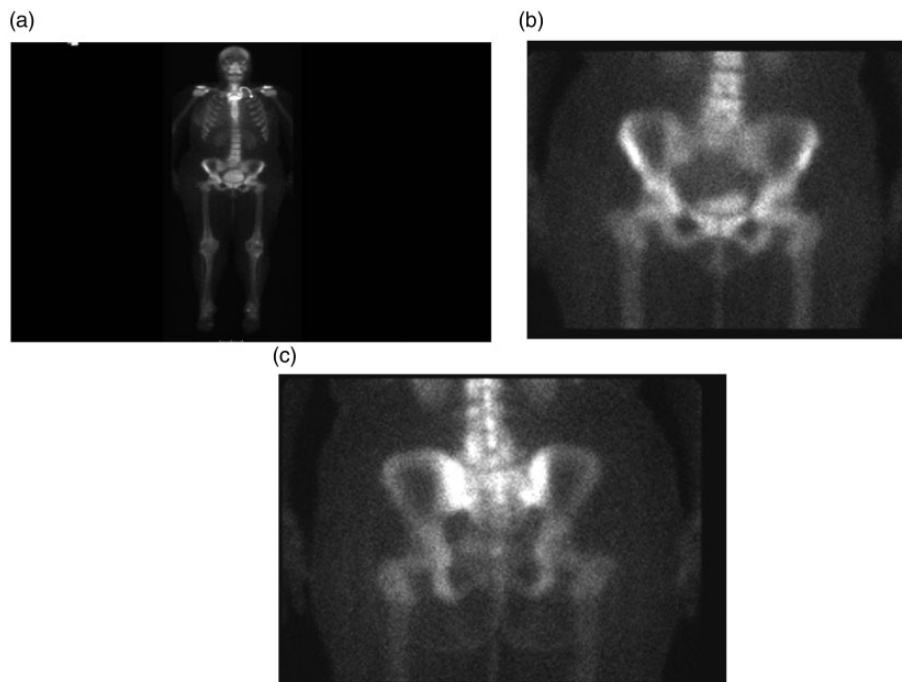


Fig. 2. (a) Tc99m MDP skeletal scintigraphy planar frontal whole-body image shows no abnormal skeletal uptake. (b) Frontal view of the pelvis shows no correlating uptake in the left sacrum suggesting absence of osteoblastic activity. (c) Posterior view of the pelvis shows no focal abnormalities.

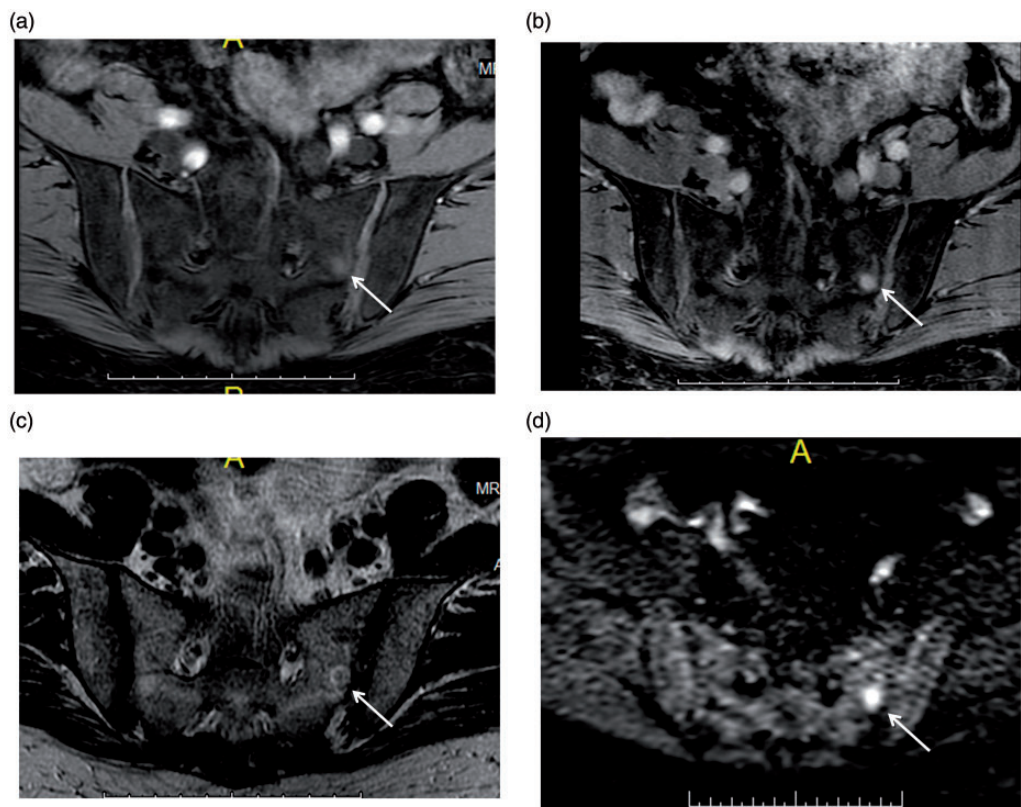


Fig. 3. Pelvic MR exam. Axial pre-contrast (a) and post-contrast (b) T1W MR images through the sacrum demonstrate a left sacral lesion that enhances after contrast administration. (c) Axial T2W MR image shows peripheral increased signal sharply demarcating the boundary of the lesion. (d) Axial high b-value ($b = 800$) diffusion-weighted image demonstrates restricted diffusion within this lesion.

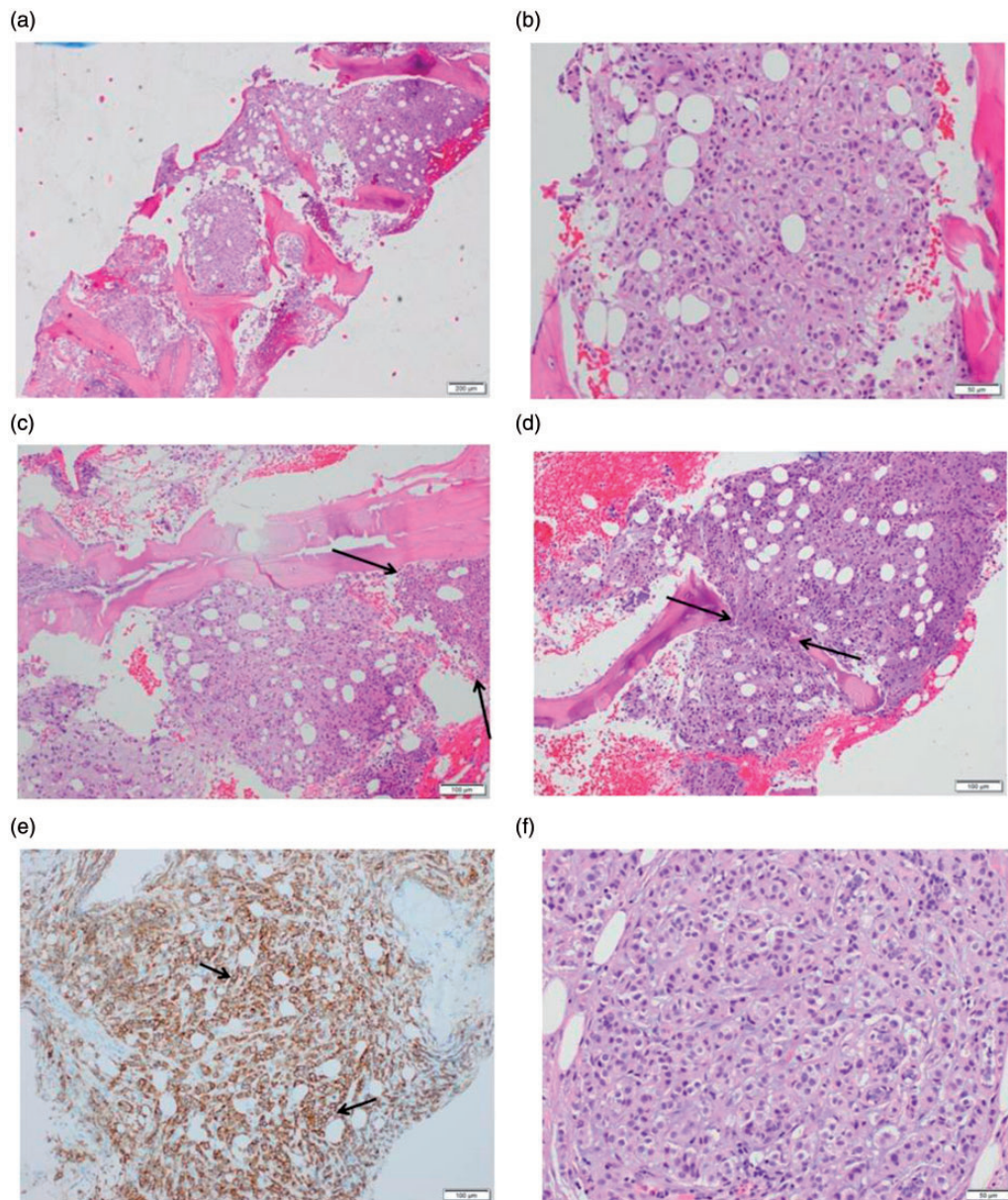


Fig. 4. (a) H&E 1× magnification sacral biopsy sample shows clusters of metastatic breast carcinoma replacing normal marrow elements. (b) H&E 20× magnification stained sample shows a neoplastic process consisting of epithelioid cells growing in cords with round monomorphic nuclei and occasional nucleoli. (c) H&E 10× magnification stained sacral core biopsy shows normal hematopoietic elements adjacent to metastatic breast carcinoma. Note the sites of tumors cells closely abutting normal marrow elements (black arrows). There is relative preservation of bony architecture, although there are scattered areas of bony trabecular destruction. (d) H&E-stained sacral core biopsy at 4× magnification shows destruction of bony trabeculae (black arrows) with surrounding metastatic carcinoma, suggest that a lytic process is also present. (e) HER2 staining shows strong membranous staining by HER2 receptor (arrows). (f) H&E-stained core biopsy of the primary breast cancer at 20× magnification shows IDC with similar morphologic features to the sacral lesion.

Yang et al. evaluated the pooled (%sensitivity, %specificity) of radiologic modalities in the detection of all bone metastases in a meta-analysis including 67 studies as follows: FDG PET (89.7, 96.8); CT (72.9, 94.8); MR (90.6, 95.4); and skeletal scintigraphy (86, 81.4) (4). FDG PET and MR showed the highest

sensitivity while CT showed the lowest sensitivity for lesion detection. However, this study incorporated a wide variety of types of malignancies. While planar skeletal scintigraphy is reported to have sensitivity between 70–90% for lesion detection, the addition of SPECT/CT raises the sensitivity up to 95% in some

series (13,14). Abikhzer et al. showed that whole body Tc99m MDP bone single-photon emission computed tomography (SPECT) had a sensitivity of 63% and specificity of 97% on lesion based analysis of bone metastases from breast cancer in 21 patients. However, serial multimodality imaging including 18F PET established the gold standard imaging in this recent study, which could explain relative sensitivity differences (15). Piccardo et al. showed that in breast cancer, FDG PET had higher sensitivity for the detection of bone metastases than MDCT (91% vs. 77%, respectively) (7). No large studies are available to discuss the effect of breast cancer histologic subtype on the multimodality imaging detection of bone metastases. However, Maffione et al. reported a case of osteoblastic skeletal metastases from invasive lobular carcinoma (ILC), which were negative on PET imaging (16). Lower FDG uptake has been suggested in ILC compared to IDC. Lower tumor cell concentrations of FDG, infiltrative spread to adjacent tissues, and decreased GLUT1 expression in ILC could explain the decreased FDG uptake (17–19).

Breast cancer tumor cells undergo an osteolytic cycle related to secretion of parathyroid hormone related peptide as a primary stimulator of osteoclastogenesis. These tumors produce other factors also increasing osteoclast activity including interleukin-6 (IL-6), tumor necrosis factor (TNF), prostaglandin E2 (PGE2), and macrophage colony-stimulating factor (M-CSF) (20). RANK ligand expression is increased and bone resorption is induced. The following bone resorption process ultimately releases factors that increase tumor growth. Earlier authors have described a symbiotic relationship between bone destruction and neoplasm growth (20). Our patient started with denosumab therapy, which prevents development of osteoclasts by inhibiting the RANK ligand to disrupt the symbiotic osteolytic cycle and prevent bone tumor growth.

In conclusion, despite the higher sensitivity of FDG PET-CT and MR for bone lesion detection in breast cancer, skeletal scintigraphy and MDCT are commonly the first step in whole-skeleton staging evaluation for breast cancer. However, FDG PET-CT or MR should be recommended in high-risk patients for further evaluation of indeterminate bony findings, which could potentially lead to pharmacotherapy changes and prevent adverse skeletal-related events. Additionally, to our knowledge this case report is the first to provide a radiologic-pathologic correlation and histologic explanation for why breast cancer bone metastases may be ambiguous on both MDCT and scintigraphy. Within the current guidelines, our case report serves as a reminder to clinicians and radiologists of the limitations of MDCT and scintigraphy in detecting subtle bone metastases.

Declaration of conflicting interests

The author(s) declared no potential conflicts of interest with respect to the research, authorship, and/or publication of this article.

Funding

The author(s) received no financial support for the research, authorship, and/or publication of this article.

References

- Hussein O, Komarova SV. Breast cancer at bone metastatic sites: recent discoveries and treatment targets. *J Cell Commun Signal* 2011;5:85–99.
- Network NCC. NCCN Clinical Practice Guidelines in Oncology. Breast Cancer Version 2.2017.
- Coleman RE, Seaman JJ. The role of zoledronic acid in cancer: clinical studies in the treatment and prevention of bone metastases. *Semin Oncol* 2001;28:11–16.
- Yang HL, Liu T, Wang XM, et al. Diagnosis of bone metastases: a meta-analysis comparing ¹⁸F-FDG PET, CT, MRI and bone scintigraphy. *Eur Radiol* 2011;21:2604–2617.
- Muindi J, Coombes RC, Golding S, et al. The role of computed tomography in the detection of bone metastases in breast cancer patients. *Br J Radiol* 1983;56:233–236.
- Davila D, Antoniou A, Chaudhry MA. Evaluation of osseous metastasis in bone scintigraphy. *Semin Nucl Med* 2015;45:3–15.
- Piccardo A, Altrinetti V, Bacigalupo L, et al. Detection of metastatic bone lesions in breast cancer patients: fused ¹⁸F-Fluoride-PET/MDCT has higher accuracy than MDCT. Preliminary experience. *Eur J Radiol* 2012;81:2632–2638.
- Heindel W, Gubitza R, Vieth V, et al. The diagnostic imaging of bone metastases. *Dtsch Arztebl Int* 2014;111:741–747.
- Cook GJ, Fogelman I. The role of positron emission tomography in the management of bone metastases. *Cancer* 2000;88:2927–2933.
- Daldrup-Link HE, Franzius C, Link TM, et al. Whole-body MR imaging for detection of bone metastases in children and young adults: comparison with skeletal scintigraphy and FDG PET. *Am J Roentgenol* 2001;177:229–236.
- Eustace S, Tello R, DeCarvalho V, et al. Whole body turbo STIR MRI in unknown primary tumor detection. *J Magn Reson Imaging* 1998;8:751–753.
- Steinborn MM, Heuck AF, Tiling R, et al. Whole-body bone marrow MRI in patients with metastatic disease to the skeletal system. *J Comput Assist Tomogr* 1999;23:123–129.
- Ghosh P. The role of SPECT/CT in skeletal malignancies. *Semin Musculoskelet Radiol* 2014;18:175–193.
- Montilla-Soler JL, Mankanji R. Skeletal scintigraphy. *Cancer Control* 2017;24:137–146.
- Abikhzer G, Srour S, Fried G, et al. Prospective comparison of whole-body bone SPECT and sodium 18F-fluoride

- PET in the detection of bone metastases from breast cancer. *Nucl Med Commun* 2016;37:1160–1168.
16. Maffione AM, Lisato LC, Rasi A, et al. Lobular breast carcinoma: a case of rare possible ¹⁸F-FDG PET/CT and bone scan false negative. *Clin Nucl Med* 2015;40: e134–136.
 17. Avril N, Rose CA, Schelling M, et al. Breast imaging with positron emission tomography and fluorine-18 fluorodeoxyglucose: use and limitations. *J Clin Oncol* 2000;18: 3495–3502.
 18. Bos R, van Der Hoeven JJ, van Der Wall E, et al. Biologic correlates of (18)fluorodeoxyglucose uptake in human breast cancer measured by positron emission tomography. *J Clin Oncol* 2002;20:379–387.
 19. Buck AK, Schirrmester H, Mattfeldt T, et al. Biological characterisation of breast cancer by means of PET. *Eur J Nucl Med Mol Imaging* 2004;31(Suppl. 1): S80–87.
 20. Roodman GD. Mechanisms of bone metastasis. *Discov Med* 2004;4:144–148.